Towards stable cyanobacterial cell factories

Du, W.

Publication date
2018
Document Version
Other version
License
Other

5 Growth-coupled photosynthetic fumarate production in cyanobacteria

Genetically engineered cyanobacterial cell factories may have the ability to use sun(light) to recycle CO_2 directly into diverse compounds. Yet, an unexpected drop in productivity has occasionally been reported, which could compromise the viability of scale-up of this sustainable conversion process. We have recently demonstrated that a stable productivity may be achieved if production strains are engineered to align biomass and product formation. Thus far, this has only been experimentally performed in cyanobacteria for the production of acetate. Although establishing a solid proof-of-concept, for that particular product the carbon partitioning between product and biomass was found to be rather low (< 5%). According to that same study (Chapter 4) the same metabolic engineering approach could also be used to achieve the stable production of 8 more compounds in addition to acetate. In this study, we shifted the focus to another product from this list – fumarate – a compound with a variety of potential applications, which is predicted to be produced with a much higher level of carbon partitioning in a growth-coupled fashion. Here, we experimentally tested and confirmed this prediction in *Synechocystis* sp. PCC6803 (hereafter, *Synechocystis*). This was accomplished by blocking the fumarate re-utilization reaction, such that fumarate produced as a side-product of anabolism, accumulates and is ultimately exported out of the cell. Furthermore, we found that *Synechocystis* has limited ability to take up fumarate from the environment, which is a factor that contributed positively to the extracellular fumarate accumulation. With 20~30% of carbon partitioning, the rate of fumarate production, is found to be proportional to growth rate, *i.e.* these two phenotypic traits are coupled. The stability of the newly engineered production strain was tested in prolonged turbidostat cultivations (*i.e.* for over 25 days). Fumarate productivity remained stable, while a strain engineered using classical strategies, which initially displayed a comparable carbon partitioning, lost its ability to form product within 5 to 10 days. With the present study we have pushed the bar in terms of what is deemed possible in terms of carbon partitioning in growth-coupled engineered strains, representing a significant step towards the development of stable cyanobacterial factories.

This chapter forms the basis of a manuscript in preparation:

Du, W., Jongbloets, J.A., Hellingwerf, K.J., Branco dos Santos, F., (2017) Growth-coupled photosynthetic fumarate production in cyanobacteria.

5.1 Introduction

The unpredictability of the production process, that emerges from the instability of engineered strains in production settings, is one of the major technical hurdles of biotechnology [38,71,176]. This instability occurs because the most commonly used metabolic engineering approaches make cells that produce a specific product in direct competition with biomass formation, which imposes a high fitness burden on production strains. This ultimately leads to a rapid appearance of suppressor mutations, for instance in the form of insertions or deletions, that impair the culture's ability to form product [134,177]. So-called "growth-coupled production" (*i.e.* obligate coupling of the synthesis of specific target products with bacterial growth) can help stabilize production traits: When the formation of product and biomass are aligned (*i.e.* obligatorily coupled), non-producing mutants that emerge spontaneously are outcompeted by the fitter producing strains according to Darwinian selection principles [137]. The theoretical framework behind the engineering of growth-coupled strategies has thus far been underpinned by a common principle - linking a product-forming pathway to the capacity of the cell to regenerate energy and/or redox co-factors. This principle has been proposed to hold for photoautotrophs but was so far never successfully implemented in the laboratory [147]. This might be caused by the plasticity conferred to cyanobacteria by all the alternative electron flows surrounding the photosystems I and II, which makes it very difficult to achieve the desired strict coupling [18].

The innovative metabolic engineering strategy proposed in Chapter 4 of this thesis may help take this hurdle. In this chapter, we have developed a method to design growth-coupled production strategies based on a new principle. Instead of using energy or redox regeneration, this is now based on the direct stoichiometric coupling of pathways uniquely responsible for the formation of biomass precursors to the production of target compounds. This is achieved through the deletion of the native metabolic route(s) that cells have to reintroduce side-products back into anabolism. Such deletions lead to the accumulation of these side-products, and hence, ensure their growth-coupled production. In order to identify suitable metabolic intermediates that are a suitable target, this concept has been developed into an algorithm that can be used to "Find Reactions Usable In Tapping Side-products" - FRUITS. By analyzing existing genome-scale metabolic models, this open source pipeline identifies anabolic side-products that can be coupled to cell growth by the deletion of their re-utilization pathway(s). The number of products that will be identified this way will depend on the number of gene deletions (aimed to remove salvation pathways) that one allows. When applied to *Synechocystis* growing under photoautotrophic conditions, FRUITS predicts that nine compounds can be coupled to growth with a maximum of four gene deletions.

In chapter 4 we have validated this approach with the production of acetate. Here, we have shifted the focus to another product of the list of compounds – fumarate – as our simulations indicate that it will be produced in much larger amounts (> 4-fold; and an independent report has made a somewhat similar prediction [145]).

Fumaric acid (fumarate of its dissociated form) is a C4 carboxylic acid with multiple applications across diverse fields. As a relatively cheap nontoxic acid (it belongs to the GRAS — generally recognized as safe - category), fumaric acid has long been used as an acidity regulator in the food industry [178]. Due to its double bond and two carboxylic acid groups, fumaric acid is a suitable building block for polymer (*e.g.* biodegradable plastic) production [179]. Consequently, fumaric acid has been designated by the US Department of Energy as a Top 12 green commodity chemical, which indicates its potentially high market volume [158]. Additionally, fumaric acid functions as a medicine to treat psoriasis and as a supplement in cattle feed to reduce methane emissions [180]. Thus far, the majority of fumaric acid is produced from refined fossilized carbon deposits by chemical synthesis. Given the aforementioned applications of fumaric acid, a sustainable and bio-based route for its production would be relevant.

The analysis of the genome-scale metabolic model (GSM) of *Synechocystis* sp. PCC6803 (hereafter, *Synechocystis*) constrained to simulate photoautotrophic growth, reveals that fumarate is produced as a by-product of specific anabolic reactions within purine- and urea metabolism and is re-assimilated through the TCA cycle via the activity of FumC (fumarase) (Fig 5.1A). If the only fumarate assimilation pathway present is removed, by the construction of a *fumC* deletion strain, FRUITS predicts that fumarate will accumulate at a yield of 0.848 mmol fumarate per gDW. In this study, we directly test this prediction by constructing a Δ*fumC Synechocystis* mutant (Fig 5.1B). While the precise compartment in which the produced fumarate accumulates is not important *in silico*, the actual compartment (*i.e.* the cytoplasm, periplasm or the extracellular volume) is unknown in *Synechocystis.* We therefore also used this newly constructed strain to perform preliminary experiments to elucidate the native capacity of these cells to transport fumarate. Furthermore, we studied the relationship between the rates of fumarate productivity and growth rate. The results of these experiments confirmed the efficacy of this metabolic engineering strategy in stabilizing production also for a strain with a moderate carbon partitioning (> 20%) even during prolonged cultivation. To the best of our knowledge, this is the first report of growth-coupled photosynthetic fumarate production in cyanobacteria and the highest carbon partitioning ever reported for any product produced via this approach.

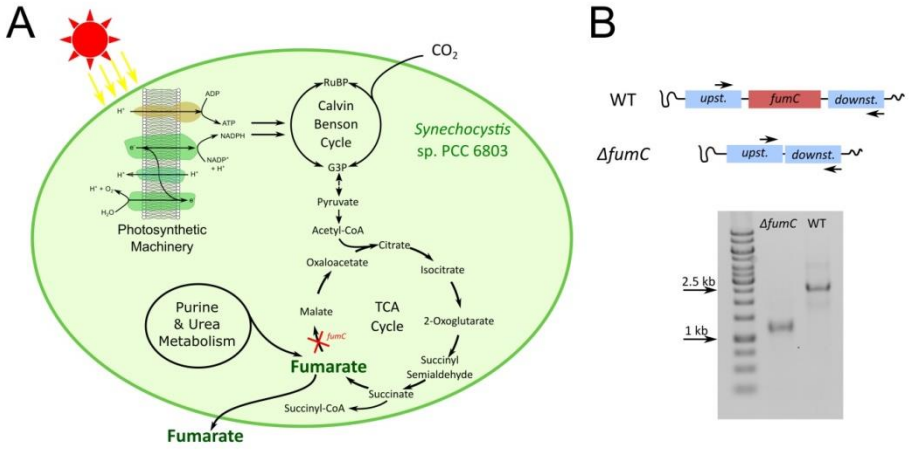

Figure 5.1. Schematic representation of fumarate metabolism in *Synechocystis*. (A) A deletion of *fumC* (red X) in the TCA cycle blocks fumarate re-utilization, thereby enabling its accumulation. (B) PCR confirmation of the *ΔfumC* mutant. With the primers indicated (black arrows), a clean knockout of *fumC* gives a single DNA band ~ 1.2 kb, while the corresponding fragment for wild type (WT) is ~ 2.5 kb. Abbreviations: RuBP, Ribulose-1,5-bisphosphate; G3P, Glyceraldehyde 3-phosphate.

5.2 Results and Discussion

5.2.1 Extracellular fumarate production by a *Synechocystis fumC* deletion strain

We used a clean *Synechocystis fumC* deletion mutant (*ΔfumC*) to experimentally test its capacity to produce fumarate, using the wild type *Synechocystis* as a control. Under constant illumination, *Synechocystis* wild type and the *ΔfumC* strain grew similarly during the exponential growth phase. Wild type reached a slightly higher optical density after entering stationary phase (Fig. 5.2A). Not surprisingly, there was no extracellular fumarate production in *Synechocystis* wild type. In contrast, the *ΔfumC* strain excreted significant amounts of fumarate throughout the cultivation (> 1 mM final concentration; see Fig. 5.2B). These results very nicely match the *in silico* prediction that disrupting *fumC* will result in fumarate accumulation.

How fumarate was transported across plasma membrane of *Synechocystis* is currently unknown. What we observed here for Δ*fumC* is a net extracellular accumulation of fumarate, implying that ultimately fumarate secretion is faster than its uptake. It would, however, be interesting to know how much (if any) of the fumarate that is excreted can be taken up again by the cells.

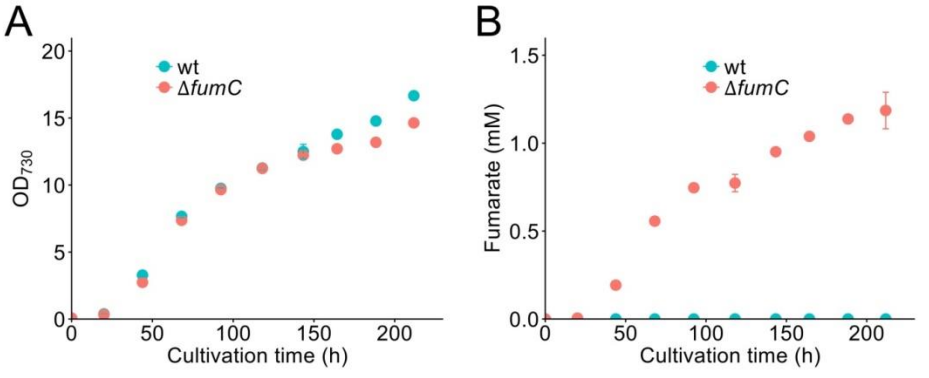

Figure 5.2 Cell growth and extracellular fumarate production in different *Synechocystis* strains. (A) Cell growth of both wild type and the ***ΔfumC*** strain in a Multi-Cultivator illuminated with constant light for over 200 hours. (B) Extracellular fumarate production for both strains. Error bars indicate the standard deviations (n=2). If an error bar is not visible, it is smaller than the size of the symbol.

5.2.2 Restricted fumarate assimilation in *Synechocystis*

To test whether *Synechocystis* carries an import system to effectively assimilate fumarate, exogenous fumarate (5 mM) was added to the cultures of both wild type and Δ*fumC*. Under constant illumination in a controlled atmosphere of 1% CO_2 and 99% N_2, no significantly different growth behavior was observed between these two strains (Fig 5.3A). Regarding fumarate assimilation, although there seemed to be a slight (albeit statistically non-significant) fumarate decrease for both strains, the fumarate concentrations for wild type remained relatively stable afterwards, while for the Δ*fumC* strain, extra (*i.e.* growth-coupled) fumarate production was observed (Fig 5.3B). These results are in sharp contrast to the results we obtained for acetate where external acetate was clearly assimilated in *Synechocystis* wild type (Chapter 4). This indicates that both wild type and Δ*fumC* may lack the ability to assimilate fumarate, under the conditions tested, or at the very least that the rate of the latter process is severely restricted. Our results thus strongly hint to the absence of a fumarate import system in *Synechocystis*.

It is a bit counterintuitive that *Synechocystis* would be unable to efficiently assimilate external fumarate. Fumarate serves as an important metabolite in the TCA cycle, and its synthesis from CO_2 costs a considerable amount of energy (*i.e.* much more than the energy required for the uptake process). This seemingly paradoxical behavior has also been reported for both *Synechocystis* and *Synechococcus* sp. strain PCC 7942 for yet another TCA cycle intermediate - 2-oxoglutarate [181,182]. For both cyanobacterial species,

exogenous 2-oxoglutarate was barely assimilated by cells, as concluded from the absence of a significant stimulatory growth effect. However, when a heterologous 2-oxoglutarate influx transporter (from *E.coli*) was expressed in both strains, even 1 mM of external 2-oxoglutarate added to the cultures caused a detrimental effect on cell growth. It could be that uptake of fumarate is also somewhat toxic to *Synechocystis*. In order for cells to prevent such toxicity effects, a lack of an import system would minimize the risk of intracellular fumarate accumulation. Our observation in *Synechocystis* is clearly distinct from those made with chemotrophic bacteria, such as *E.coli,* which has a complicated regulation system to take up fumarate under different levels of oxygen supply [183]. Noteworthy, only 6% of the putative transporters encoded in the chromosome of *Synechocystis* are predicted to facilitate transport of carbon compounds, in comparison with 28 and 20% in *E. coli* and *B. subtilis*, respectively [184]. This further supports the idea that a deficiency of import systems in *Synechocystis* is a defense mechanism, because of a putatively low tolerance to fumarate.

5.2.3 Low fumarate tolerance of *Synechocystis*

To determine how much fumarate *Synechocystis* can tolerate, different amounts of external fumarate were supplemented to cultures of both wild type and Δ*fumC*, while their final cell densities were monitored. With a custom developed 96-well microplate system [185], a range of fumarate concentrations up to 150 mM were tested. Up to a fumarate concentration of 16 mM, no significant inhibition of cell growth was observed for both strains, although wild type reached a higher cell density compared with Δ*fumC* (Fig 5.3C). This result is consistent with the previous results shown in Fig 5.2A, where wild type also reached a higher cell density at the end of the cultivation. The reason could be either that fumarate production in Δ*fumC* affects the yield of inorganic carbon on biomass, especially at high OD values when inorganic carbon is limiting, or higher maintenance requirements in Δ*fumC,* possibly due to fumarate toxicity. When the amount of supplemented fumarate was > 31 mM, both wild type and Δ*fumC* showed significant growth retardation, both to a similar level, indicating that at these concentrations fumarate becomes toxic.

These results raise an interesting question: why was cell growth inhibited by the external fumarate supplemented at a relatively low concentration if cells have restricted uptake capacity [186,187]? There are several possible explanations. First is the pH of the medium after adding different amount of fumarate. However, given the buffer capacity of the medium relative to the amounts of di-sodium fumarate added, the predicted fluctuation in pH will be very small [188] and hard to account for the differences observed. Secondly, the chelation of iron ions by fumarate may restrict cells to get access to the iron.

Ferrous fumarate has been reported to have low solubility at pH 6, compared to pH 2 [189]. Its solubility is even lower at pH 8, which could decrease the availability of free ferrous ions in the solution. However, the actual form of iron in the medium is ferric, which fumarate does not seem to chelate. Nonetheless, ferric ions are converted to ferrous ions before they enter the cells. Last but not least, similar toxicity effects could be expected for fumarate as to 2-oxoglutarate, such as imbalance of metabolites *etc.*

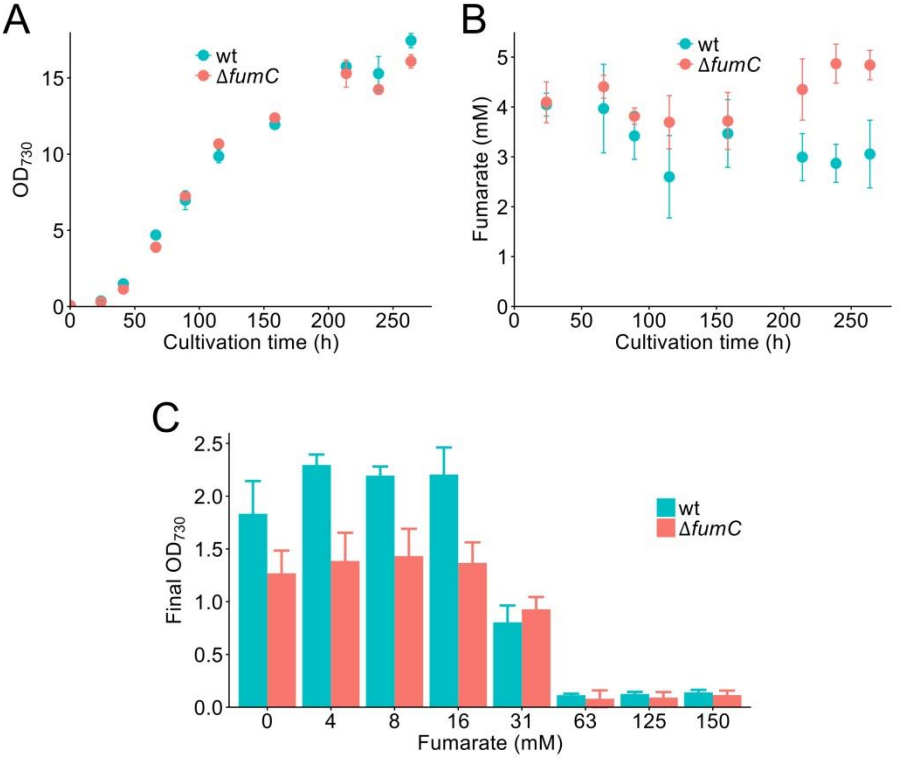

Figure 5.3 Characterization of fumarate assimilation and tolerance in different *Synechocystis* strains. (A) Cell growth of both wild type and Δ *fumC* in Multi-Cultivator under constant light illumination for over 200 hours, where about 5 mM di-sodium fumarate was supplemented in the medium. (B) Fumarate levels along the whole cultivation. (C) Final OD for both strains after about 50 hours of cultivation in a custom developed microplate system. Error bars indicate the standard deviations (n=2 for A & B, n=6 for C). If an error bar is not visible, it is smaller than the size of the symbol.

Although at an external fumarate concentration of 31 mM this dicarboxylic acid starts to inhibit cell growth, to achieve such a high titer in a *Synechocystis* culture still presents a big challenge. Overcoming this challenge depends not only on the possibility to reroute a higher carbon flux towards fumarate synthesis, but equally important, to maintain stable fumarate productivity.

5.2.4 Fumarate production rate is proportional to growth rate

While undoubtedly promising, these initial simple growth experiments do not assure that biomass and fumarate formation are strictly coupled. The strict stoichiometric coupling, which we are striving to engineer, implies that at different growth rates one would expect a linearly proportional change in the biomass specific production rate of fumarate. The latter still remained to be tested with this initial set of experiments alone.

We tested whether fumarate production and growth rate strictly vary in parallel in the *ΔfumC* strain, by performing 12 independent photonfluxostat experiments at different, yet constant, growth rates [164]. This was achieved by dosing the biomass specific light flux to intensities ranging from 30 to 100 µmol photons m^{-2} s^{-1} OD^{-1}. From all cultivations maintained at a specific growth rate, samples were taken at different sampling times, to quantify extracellular fumarate concentration. Fumarate productivities were subsequently calculated and plotted against growth rate (Fig. 5.4A). The results obtained indicate that fumarate productivity is indeed proportional to growth rate, implying that both physiological traits are indeed strictly coupled. Furthermore, we compared the linear fit between the rate of fumarate productivity and growth rate, based on our experiments, with the outcome of the simulations using FBA on the metabolic network reconstruction of *Synechocystis*. It is important to highlight that we did not in any way tweak the modeling parameters, which were taken directly from the original report [18]. Still, both sets of data match strikingly well, corroborating that indeed the hypothesis that fumarate production and growth rate are strictly coupled in the *ΔfumC* strain seems to hold up to scrutiny.

We also calculated the carbon partitioning towards fumarate in the *ΔfumC* strain during the multiple cultivations carried out (Fig 5.4B). This was calculated based on the average optical density and fumarate concentration, between each two subsequent sampling points. Optical density was converted to gram of dry biomass based on a previous report [164]. The plotted carbon partitioning is an average of individual values obtained for each time interval with standard deviation. We did not see any significant changes in carbon partitioning irrespective of the biomass specific light flux (Fig 5.4B). This indicates that irrespective of the growth rate, as long as cells are illuminated, the fumarate yield on biomass is constant. This result also supports theoretical predictions stating that fumarate production is only affected by environmental conditions to the extent that the latter affect growth rate. In other words, fumarate production is stoichiometrically and obligatorily coupled to growth. It is important to note that the carbon partitioning values reported here are comparable with most of those obtained using more conventional metabolic engineering strategies for a wide variety of products [72].

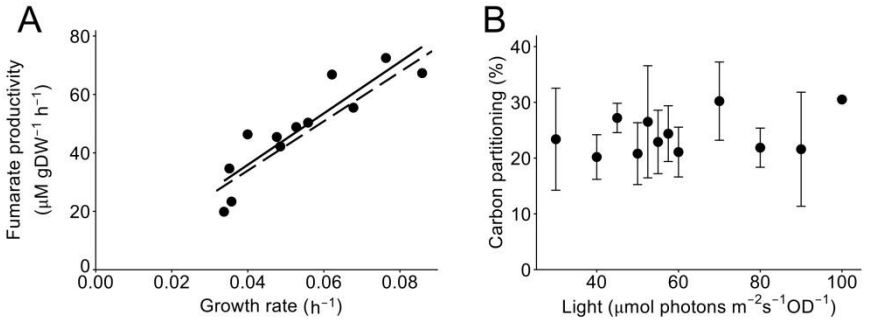

Figure 5.4 Strict coupling relationship between growth rate and rate of product formation in the *ΔfumC* strain. (A) A linear relationship between growth rate and biomass specific fumarate productivity. Each point represents a single observation, and the solid line is a linear fit of all experimental data points. The dashed line is based on *in silico* FBA simulations of the genome-scale metabolic model of *Synechocystis,* using biomass maximization as the objective function. (b) Carbon partitioning of fumarate production versus biomass at different light regimes (or: growth rates; see text). Error bars indicate the standard deviation of carbon partitioning calculated at times throughout the cultivation (n>3).

5.2.5 Stability of fumarate production by the *ΔfumC* strain

The *ΔfumC* strain is producing fumarate in a growth-coupled fashion, but whether this does indeed improve the phenotypic stability of the production trait remains to be tested. As explained above, the root of the instability comes from Darwinian selection for fitter (*i.e.* faster growing under the selected conditions) strains. When using classical metabolic engineering strategies, the fitter strains are the non-producing ones; when using our new growth-coupled strategy, it should be the producing ones (at least while cells do not re-evolve a new fumarate assimilation pathway, which we do not expect to be a very likely event on the short-term). Conditions in which cells are under a strong selection pressure for fastest growth and in which the propagation bottlenecks are smallest, are predicted to result in the fastest drop in productivity [190]. Such conditions, while maintaining the total population size relatively constant, are best met under turbidostat cultivation [97], and so these cultivations provide the harshest test ground to assess the stability of our production strains.

We cultivated the *ΔfumC* strain under turbidostat conditions at the maximal growth rate (i.e. without light limitation), for a period of over 600 hours. During this period we did not observe any significant changes in production rate (Fig. 5.5A) - a true testament to the stability of our fumarate producing strain. As a control, we compared how a *Synechocystis* strain that was engineered using classical approaches to produce lactate [55] fairs under the same conditions. Lactate production in this strain was achieved by the heterologous expression

of lactate dehydrogenase from *Lactococcus lactis*, yielding an initial carbon partitioning similar to the one here reported for fumarate. As theory would predict, lactate production was lost within 5 to 10 days for a culture of this strain (Fig. 5.5B). This result reinforces the stringency with which this regime selects for fitter cells, which - when using our novel engineering method - means the producing ones.

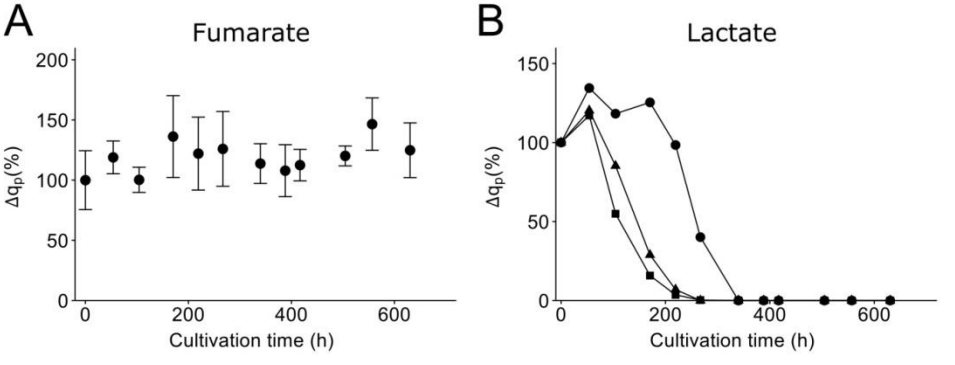

Figure 5.5 Stability of production of fumarate (A) and lactate (B) during prolonged turbidostat cultivation under continuous illumination. For fumarate, productivity at corresponding time points was normalized based on the average productivity at the first time point (set to be 100%). The error bars indicate the standard deviation of 4 replicates. For lactate, each symbol represents a single observation normalized by its first time point (set to be 100%). The initial burden of deviating carbon from biomass formation (*i.e.* % carbon partitioning) for both products is comparable.

5.3 Conclusion

Enforcing obligate coupling of cell growth with formation of a desired product is an approach to alleviate or prevent the instability of engineered strains, and thereby, can stabilize productivity. For cyanobacteria which have been extensively genetically engineered for formation of a diverse range of products, the idea of growth-coupled product formation has been proposed but not yet successfully tested experimentally by others [148,191,192]. Here, the model guided metabolic engineering strategy to achieve stable growth-coupled production of fumarate in the cyanobacterium *Synechocystis* has been successfully implemented and validated. This has been achieved via a knock-out of the product- (*i.e.* fumarate) assimilating reaction present in *Synechocystis*. Hence, the production of fumarate, which is synthesized as a side-product of anabolism, becomes stoichiometrically and obligatorily coupled to growth of the organism. Our results show that fumarate, that initially, accumulates in the cytoplasm, can be secreted (even though the molecular mechanism of this

process is still unknown) to the extracellular space, while external fumarate cannot be efficiently re-assimilated. Such a transport phenotype fits well with the development of photosynthetic cell factories as products will remain in the supernatant of the culture, which is more accessible for downstream processing. Although a relatively low tolerance to fumarate was observed, achieving such a titer, particularly in an industrial setting still seems unlikely, and besides, improvement of product tolerance has precedents in cyanobacteria [193]. Nonetheless, ultimately, we provide compelling evidence that (i) the *ΔfumC* strain produces fumarate; (ii) it does so in a growth-coupled fashion; and (iii) this approach stabilizes the production trait of the strain. This is the first report of fumarate production directly from CO_2 using an engineered cyanobacterium and the highest carbon partitioning achieved in photoautotrophic cell factories that has been demonstrated to be stable during prolonged cultivation.

5.4 Materials and methods

5.4.1 Strains and general cultivation conditions

Molecular cloning was performed in *E. coli* DH5α growing either in liquid Luria-Bertani (LB) broth at 37 °C incubator with a shaking speed of 200 rpm, or on solidified LB plates containing 1.5% (w/v) agar. Antibiotics were added, when appropriate, in the medium for propagation of a specific plasmid. Concentrations of antibiotics used, alone or in combination, were 100 μg mL^{-1} for ampicillin and 50 μg mL^{-1} for kanamycin.

Glucose-tolerant *Synechocystis* was obtained from D. Bhaya, University of Stanford, Stanford, CA. Normal cultivation was performed in BG-11 medium at 30 °C inside an incubator shaking at 120 rpm (Innova 43, New Brunswick Scientific), under constant moderate white-light illumination (~30 μmol photons m^{-2} s^{-1}, measured with a LI-250 light meter). For *Synechocystis* mutant construction, we added kanamycin or nickel sulfate to the medium with a final concentration of 50 μg mL^{-1} or 20 μM, respectively. Cell growth was quantified through measurement of the optical density (OD) at 730 nm wavelength (lightwave II, Biochrom).

5.4.2 Plasmids and strains construction

All plasmids, strains and primers are listed in Table 5.1. For the marker-less deletion of a gene in the *Synechocystis* chromosome, two plasmids were required. Plasmid one contains up- and down- homologous regions (~1 kb each) of the target gene, while the second plasmid has an extra selection cassette flanked between both homologous regions. The selection cassette consists of a kanamycin resistance fragment and a nickel-inducible *mazF* expression fragment. As an endoribonuclease that cleaves mRNA at the ACA triplet sequence, MazF acts as a general inhibitor for the synthesis of all cellular proteins [173]. For *fumC* gene knock out plasmids, each homologous region was amplified by PCR, using genomic DNA of *Synechocystis* as a template. The two

fragments were fused together and completely amplified through *Pfu* DNA Polymerase (Thermo Scientific). The resulting blunt DNA fragment was purified with a gel extraction kit (Zymo Research), and attached with one extra adenosine ("A") of its 3' overhang by *Taq* DNA Polymerase (Thermo Scientific). Through TA cloning, target fragments with an extra "A" were ligated to the BioBrick "T" vector pFL-AN [182], resulting in pWD060. Due to the extra XbaI restriction site introduced through primers between two homologous regions, a selection cassette with XbaI on both sides (from pWD42) can be easily inserted into pWD60. The resulting plasmid is named pWD061. All the fragments amplified in this study were confirmed by Sanger sequencing at Macrogen Europe (The Netherlands).

Table 5.1 Plasmids, strains and primers used in this study

Plasmids, stains and primers[#]	Relevant characteristics	Reference
pFL-AN	BioBrick "T" vector with AvrII and NheI on each side	(182)
pWD42	Amp^rKm^r, containing selection cassette	(175)
pWD060	pFL-AN derivate, Amp^r, containing *fumC* gene upstream and downstream homologous regions	This study
pWD061	pFL-SN derivate, Amp^rKm^r, containing *fumC* gene upstream homologous region, selection cassette, and downstream homologous region	This study
Synechocystis sp. PCC6803	*Synechocystis* sp. PCC6803 wild type	D. Bhaya
Δ*fumC*	*Synechocystis* sp. PCC6803 *fumC* gene knock out mutant	This study
fumC-up-Fwd	GAGCAGACGTTCACATCG	This study
fumC-up-Rev	CAATCATCTGCTCTGGAACGtctagaCATACTGTC GGTTTCAAGGC	This study
fumC-down-Fwd	GCCTTGAAACCGACAGTATGtctagaCGTTCCAGA GCAGATGATTG	This study
fumC-down-Rev	CCTAGATTAGGACCTGTCAGC	This study
fumC-seq	AACCATTGTCCAAGGTCTGCG	This study

[#] primer sequences are given from 5'→3'

Construction of the *Synechocystis* Δ*fumC* mutant requires two rounds of transformation, as previous reported [28]. In the first round the selection cassette was integrated into the chromosome. The second round is to remove the selection cassette. Briefly, for both rounds of transformation, corresponding *Synechocystis* cells were collected either directly from plate or from liquid culture. After being washed twice with fresh BG-11 medium through centrifugation at 5,000 rpm for 5 min, cells were further concentrated to a total liquid volume of 200 µl (OD_{730} ≈ 2). Either pWD61 (first round) or pWD060 (second round) was mixed with cells to a final concentration of 10 µg mL^{-1}, then the mixture was illuminated under moderate light (~ 30 µmol photons m^{-2} s^{-1}) for 4 to 6 hours. Next, the mixture was spread on a commercial membrane (Pall Corporation),

resting on the BG-11 plate, with neither kanamycin nor nickel sulfate. After further illumination for 16~24 hours, the membrane with the mixture of cells was transferred to another BG-11 plate with kanamycin (first round) or nickel sulfate (second round). After about one week, the colonies that appeared were picked and scratched sequentially on a new BG-11 plate with kanamycin or nickel sulfate, respectively. Colonies which grow on a BG-11 plate with kanamycin but not with nickel sulfate (first round), or on BG-11 plate with nickel sulfate but not kanamycin (second round) are candidates for PCR confirmation (with 35 cycles). Further segregation by serial dilution in liquid culture was applied when necessary.

5.4.3 Batch and photonfluxostat cultivation

Batch cultivation was performed in a Multi-Cultivator (MC1000-OD, PSI, Czech Republic), with light supplied by a "cool-white" LED panel (PSI, CZ) and of which the output intensity was controlled. BG-11 supplemented with 10 mM TES-NaOH (pH = 8.0) was used for *Synechocystis* cultivation at 30 ºC and bubbled with a mix (v/v) of 99 % N_2 and 1% CO_2 at a flow rate of ~150 ml min^{-1}. Exogenous di-sodium fumarate (Sigma-Aldrich) was added in the fumarate re-assimilation experiments. The pre-cultures (OD_{730} ≈ 2) from shake flasks were used for inoculation of the Multi-Cultivator cultures, with an initial OD_{730} of 0.05 and a working volume of 60 ml. Continuous light was supplied at a fixed light intensity of 30 µmol photons m^{-2} s^{-1} after inoculation, and 120 µmol photons m^{-2} s^{-1} when OD_{730} reached 0.5. Samples were taken daily, where OD was recorded and supernatant was prepared.

Concerning photonfluxostat experiments [164], a cultivation approach to control cell growth at different yet constant growth rates, all the cultivation conditions are the same as batch cultivation except for the light intensity settings. Light intensity was 30 µmol photons m^{-2} s^{-1} after inoculation. When OD_{720} (measured through the build-in OD sensor of the Multi-Cultivator at 720 nm) was above 0.6, light intensity was automatically adjusted every 5 min to ensure light intensity per OD_{720} was constant. This light regime was maintained until maximum capacity of the LED panel was reached. Specifically, the light regimes applied were 32.5, 35, 37.5, 42.5, 45, 52.5, 55, 57.5, 70, 80, 90, 100 µmol photons m^{-2} s^{-1} OD^{-1}. In the photonfluxostat mode, a "steady-state" would be achieved and a constant growth rate can be reliably obtained. Samples were taken every a few hours during this phase, where OD_{730} was measured and fumarate concentration was quantified.

5.4.4 Prolonged turbidostat cultivation

We studied the genetic stability of our strains in populations maintained under turbidostat conditions [97]. In this continuous cultivation method, microbial populations are kept at a fixed biomass density by diluting the culture with fresh medium at the same rate as the populations grows. This feedback loop applies a strong selection pressure on cells to grow at the maximal specific growth rate achievable. The turbidostat setup used in this experiment is based on a modified Multi-Cultivator, equipped with additional pumps (Reglo ICC, ISMATEC, Germany) for the transfer of fresh medium to the cultures, and subsequently, to a waste container (*i.e.* as in a classical chemostat). The

"pycultivator" software package that controls the Multi-Cultivator and adjunct hardware, activates the pumps to dilute the cultures if the selected OD_{720} threshold is reached [164]. Cells from pre-cultures in shake flasks were inoculated at OD_{720} ~0.05 in 4 independent cylindrical vessels of the Multi-Cultivator, using the same conditions as specified before, except for the incident light intensity, which was fixed at 100 µmol photons m^{-2} s^{-1}. The OD_{720} was recorded every 5 min. When the threshold of OD_{720} > 0.6 was reached, cultures were diluted by 8% (v/v) with fresh BG11. Strain stability was assessed by monitoring growth rate and fumarate- and lactate-production at regular time points. Samples for exometabolite production were collected periodically throughout the cultivation period. The variation in production rate, expressed in percentage, was calculated relative to the one observed at the beginning of the cultivation experiment.

5.4.5 Fumarate tolerance experiment

A previously reported 96-well microplate system with acceptable evaporation rate (≈ 0.8 µl h^{-1}) was adopted in this study [185]. Briefly, *Synechocystis* pre-cultures, grown in shake flask in the exponential phase, were used for inoculation. The initial OD_{730} was approximately 0.05 in a volume of 150 µL in each well of the transparent 96-well plate with a flat bottom (CELLSTAR, greiner bio-one). Cultures were supplemented with 50 mM $NaHCO_3$, 10 mM TES-NaOH (pH = 8.0) and required amounts of di-sodium fumarate. The final pH of each well was simulated as calculated by others [188] and found to not differ by more than 0.3 pH units (Figure 5.6). Covered with a Breathe-Easy sealing membrane (Diversified Biotech), the plate was placed on a shaking platform (MTS 2, IKA) set to a shaking speed of 600 rpm. That platform was placed inside a temperature controlled light incubator (Innova 43, New Brunswick Scientific) at 30 °C under constant light illumination at ~50 µmol photons m^{-2} s^{-1}. Ambient air was supplied inside the light incubator. OD readings were collected at desired time points in a microplate reader (FLUOstar Optima). The final OD values were calculated through background subtraction, and further converted to the values comparable to the spectrophotometer (lightwave II, Biochrom).

5.4.6 Fumarate quantification

To determine the extracellular fumarate concentration, at least a 500 µL aliquot was sampled at target time points. Cells were removed through centrifugation for 10 min at 15,000 rpm at 4 ºC. The resulting supernatant was then filtered (Sartorius Stedin Biotech, minisart SRP 4, 0.22 µm) for sample preparation. Fumarate concentration was measured by HPLC-UV/VIS (LC-20AT, Prominence, Shimadzu), with ion exclusion Rezex ROA-Organic Acid column (250x4.6 mm; Phenomenex) and UV detector (SPD-20A, Prominence, Shimadzu) at 210 nm wavelength. 10 µL of the HPLC samples was injected through an autosampler (SIL-20AC, Prominence, Shimadzu), with 5 mM H_2SO_4 as eluent at a flow rate of 0.15 ml min^{-1} and a column temperature of 45 ^{o}C. The retention time of fumarate is about 20 min in this system (Fig. 5.7).

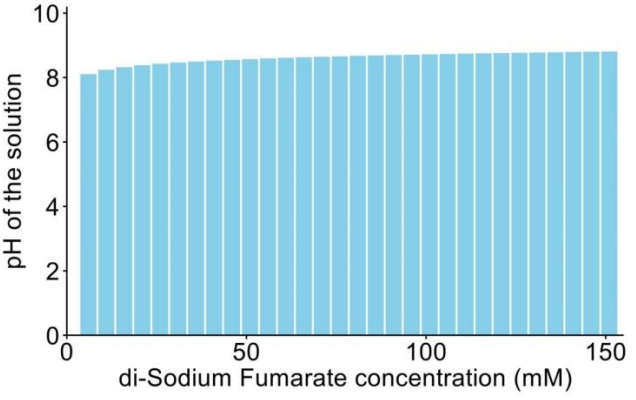

Figure 5.6 The predicted pH of the growth medium with increasing di-sodium fumarate concentrations.

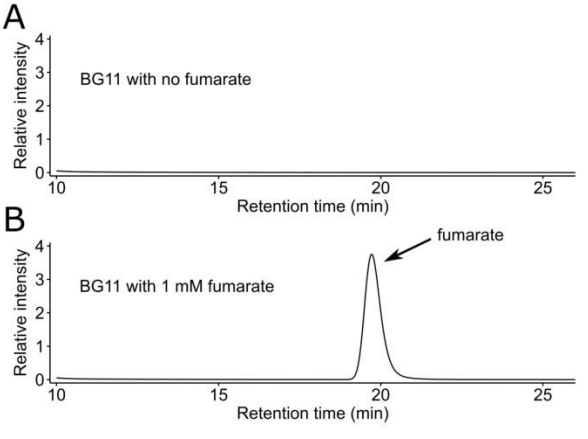

Figure 5.7 Fumarate assay using HPLC. (A) Elution curve for standard BG-11 with no fumarate addition. (B) Elution curve for standard BG-11 supplemented with 1 mM di-sodium fumarate.

5.5 Acknowledgements

The work of Wei Du was supported by the China Scholarship Council. Klaas J. Hellingwerf was supported by the Dutch Ministry of Economic Affairs, Agriculture, and Innovation (research program BioSolarCells). Filipe Branco dos Santos was supported by the Netherlands Organization for Scientific Research (NWO) through VENI grant 863.11.019.